Institute of Physics Publishing *Journal of Physics: Conference Series* **6** (2005) 73–89
doi:10.1088/1742-6596/6/1/005 *Light, Dust and Chemical Evolution*

Remote sensing of terrestrial tropospheric aerosols from aircraft and satellites

M I Mishchenko[1], B Cairns[2], J Chowdhary[2], I V Geogdzhayev[2], L Liu[2] and L D Travis[1]

[1] NASA Goddard Institute for Space Studies, 2880 Broadway, New York NY 10025, USA
[2] Columbia University and NASA Goddard Institute for Space Studies, 2880 Broadway, New York NY 10025, USA

E-mail: crmim@giss.nasa.gov

Abstract. This review paper outlines the rationale for long-term monitoring of the global distribution of natural and anthropogenic aerosols and clouds with specificity, accuracy, and coverage necessary for a reliable quantification of the direct and indirect aerosol effects on climate. We discuss the hierarchy of passive instruments suitable for aerosol remote sensing and give examples of aerosol retrievals obtained with instruments representing the low and the high end of this hierarchy.

1. Introduction

Global long-term monitoring of climate forcings and feedbacks can provide strong constraints on plausible interpretations of the observed surface temperature change and can thereby affect policy decisions with respect to environment and energy production [1]. The considerable variability of observed temperature on different time scales dictates that observations of climate forcings and feedbacks be continued for decades. The well established fact that the climate system responds to the time integral of the forcing further requires that the observations be performed continuously. These two critical requirements make long-term satellite observations the only practical means of monitoring the global climate change and its anthropogenic component provided that the measurements are sufficiently accurate [2].

Aerosol particles residing in the troposphere can cause a climate forcing directly by absorbing and reflecting sunlight, thereby cooling or heating the atmosphere, and indirectly by modifying cloud properties [3–8]. The indirect aerosol effect may include increased cloud reflectance, as aerosols lead to a larger number of cloud droplets [9], and increased cloud cover, as smaller droplets inhibit rainfall and increase cloud lifetime [10].

Unlike greenhouse gases, aerosol particles have a short lifetime in the troposphere. After they are produced they tend to mix with other agents, are transported within the troposphere both vertically and horizontally, and tend to disappear through sedimentation, rain out, etc within about a week [4]. Sulfate

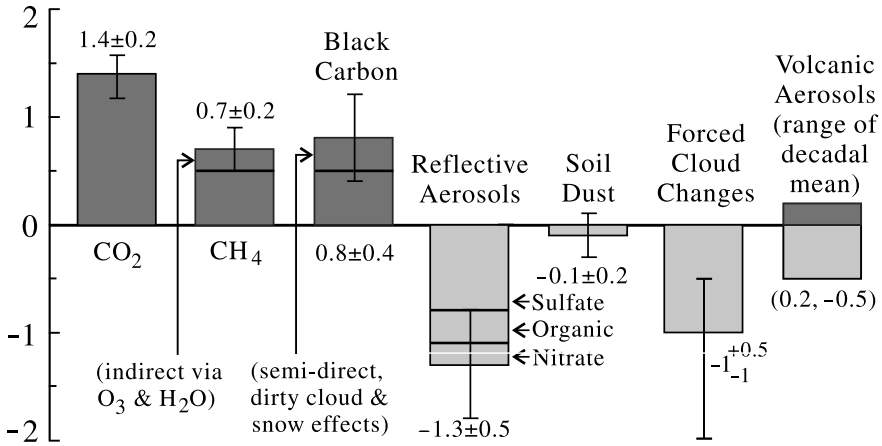

Fig. 1. The change in climate forcings by greenhouse gases and aerosols (in Wm^{-2}) during the period 1850–2000 (modified after [7]). A positive change means a contribution towards climate warming; a negative change means a contribution towards climate cooling.

particles produced by volcanos or as a result of burning sulfur-bearing fossil fuels reflect the solar radiation out into space and are believed to cause cooling of the terrestrial atmosphere. Carbonaceous aerosols result from biomass burning and industrial combustion. They absorb the solar radiation and re-radiate it at infrared wavelengths; as such they are expected to contribute to global warming. Deposits of soot particles reduce the albedo of snow and ice surfaces and facilitate the process of melting [11]. There are several other types of aerosols such as sea-salt particles from the ocean, mineral particles including desert dust, and various organic particulates. Whether they cool or warm the atmosphere depends on their microphysical properties as well as on their vertical location. Aerosol can also affect clouds and precipitation, but again the effect can be different for different aerosol species. While it is recognized that tropospheric aerosols play a key role comparable to that of the greenhouse gases (see Fig. 1(a)), the complexity and poorly understood variability of their composition and distribution in the atmosphere make it exceedingly difficult to quantify their effect on climate and weather: hotter or cooler, more rain or less, etc. Overall, the cumulative effect of the direct and indirect aerosol forcings may represent the largest uncertainty about future climate change caused by various anthropogenic activities [5–8].

Although several existing satellite instruments are used to study aerosols and their climatic effect on the global and regional scales [12–19], they remain rather limited in their ability to provide accurate particle characteristics other than the column optical thickness and an effective particle size. However, these parameters are not sufficient for an accurate quantification of the direct effect and, especially, for long-term monitoring of changes in the direct effect caused by anthropogenic factors [2]. Furthermore, the completeness and accuracy of existing and planned measurements of aerosol and cloud parameters are not sufficient for reliable evaluation of the aerosol indirect effect and its regional variations [20,21].

One of the objectives of this paper is to identify, following [22], the minimum set of measurement requirements dictated by the need to quantify the direct and indirect aerosol effects on climate and their anthropogenic components globally and with high accuracy. Another objective is to discuss the hierarchy of passive instruments suitable for aerosol remote sensing from satellites and to give examples of aerosol retrievals obtained with instruments representing the low and the high end of this hierarchy.

Table 1. Quantification of the direct aerosol effect.

Required aerosol characteristics	Retrieved aerosol characteristics	
Spectral optical thickness $\tau_a(\lambda)$	Spectral optical thickness $\tau_a(\lambda)$	For two modes
Spectral single - scattering albedo $\varpi_a(\lambda)$	Effective radius $r_{eff,a}$	
Spectral phase function $P_a(\Theta,\lambda)$	Effective variance $v_{eff,a}$	
Chemical composition	Spectral refractive index $m_a(\lambda)$	
	Nonsphericity	
	$\varpi_a(\lambda)$	

2. Measurement requirements

The left column of Table 1 summarizes the aerosol parameters that are needed for accurate global monitoring of the direct effect and its anthropogenic component [8,23,24]. All these quantities must be determined in a wide range of wavelengths λ from the near-UV to the short-wave IR. The aerosol optical thickness is usually a direct outcome of applying a retrieval algorithm to satellite data. In contrast, the single-scattering albedo, the phase function, and the chemical composition can be determined or inferred provided that aerosol microphysical parameters such as the size distribution, spectral refractive index, and shape are retrieved.

The right column of Table 1 lists aerosol parameters that must be retrieved from space in order to determine the required aerosol characteristics: the spectral optical thickness, the effective radius and effective variance of the size distribution, the real and imaginary parts of the spectral refractive index, the shape, and the single-scattering albedo. Since the aerosol population is typically bimodal (see, e.g., [25]), all these parameters must be determined for each mode.

Note that the effective radius r_{eff} has the dimension of length and provides a measure of the average particle size, whereas the dimensionless effective variance v_{eff} characterizes the width of the size distribution [26]. It has been demonstrated [26] that different types of size distribution (power law, log normal, gamma, etc.) having the same values of the effective radius and effective variance possess similar dimensionless scattering and absorption properties, thereby making r_{eff} and v_{eff} convenient universal characteristics of essentially any size distribution.

The corresponding minimum set of measurement requirements must include the retrieval of the total column optical thickness and average column values of the effective radius, effective variance, real part of the refractive index, and single-scattering albedo for each mode of a bimodal aerosol population. The optical thickness and the real part of the refractive index must be determined at multiple wavelengths in a wide spectral range, e.g., 0.35–2.5 μm. An integral part of the retrieval procedure must be the detection of nonspherical aerosols such as dust-like and soot particles. It has been demonstrated that, if ignored, nonsphericity can seriously affect the results of optical thickness, refractive index, and size retrievals [27–30].

The aerosol effect on the cloud albedo can be detected and quantified from space by means of long-term global measurements of the change in the number concentration of aerosol particles acting as cloud condensation nuclei and the associated change in the cloud albedo. Other measurable manifestations of the indirect effect include the change in the cloud droplet size and number concentration and the change

Table 2. Quantification of the indirect aerosol effect.

Required cloud and aerosol characteristics	Retrieved quantities
Cloud albedo $A_c(\lambda)$ Cloud particle effective radius $r_{eff,c}$ Cloud particle number concentration N_c Liquid water path	$\tau_c(\lambda)$ $r_{eff,c}$ $v_{eff,c}$
Aerosol particle number concentration N_a Aerosol particle effective radius $r_{eff,c}$ Aerosol chemical composition	$\tau_a(\lambda)$ $r_{eff,a}$ $v_{eff,a}$ $m_a(\lambda)$ shape For two modes

in the liquid water path [31–33]. Since the cloud condensation efficiency of aerosol particles depends on their size and hygroscopicity, the measurement of the aerosol number concentration must be accompanied by the determination of the aerosol effective radius and chemical composition.

The left column of Table 2 summarizes the cloud and aerosol characteristics that are required for reliable global monitoring of the indirect aerosol effect on climate and its anthropogenic component. The right column of this table lists the minimum set of retrievable parameters that can be used to determine the required cloud and aerosol characteristics. The respective set of minimum measurement requirements must include the retrieval of the column cloud optical thickness and the average column cloud droplet size distribution as well as the column aerosol optical thickness and the average column values of the effective radius and effective variance of the aerosol size distribution and the real part of the aerosol refractive index for each mode of a bimodal aerosol population.

Note that the cloud and aerosol particle number concentrations listed in the left column of Table 2 are derived rather than directly retrieved quantities, i.e., deduced from the column optical thickness and the particle extinction cross section (a function of size distribution, refractive index, and particle shape). Indeed, the only way to retrieve the number N of tropospheric aerosols or cloud droplets in the vertical column of unit horizontal cross section is to divide the retrieved cloud/aerosol optical thickness τ by the respective average extinction cross section per particle, C_{ext}. The strong dependence of the extinction cross section on the effective radius (Fig. 2) and effective variance makes the retrieval of the cloud and aerosol number concentrations very difficult and necessitates the determination of the respective size distributions with accuracy unattainable with instruments based on radiometric measurements alone (see [34,35] and Section 5). Assuming rather than retrieving the effective variance of the cloud droplet and aerosol size distributions can further increase the errors in the retrieved number concentrations.

3. Measurement accuracy requirements

The criteria for specifying the corresponding measurement accuracy requirements must be based on the requisite ability to detect plausible changes of the aerosol radiative forcing estimated to be possible during the next 20 years and to determine quantitatively the contribution of this forcing to the planetary energy balance. A significant global mean flux change can be defined as 0.25 Wm^{-2} or greater based on the

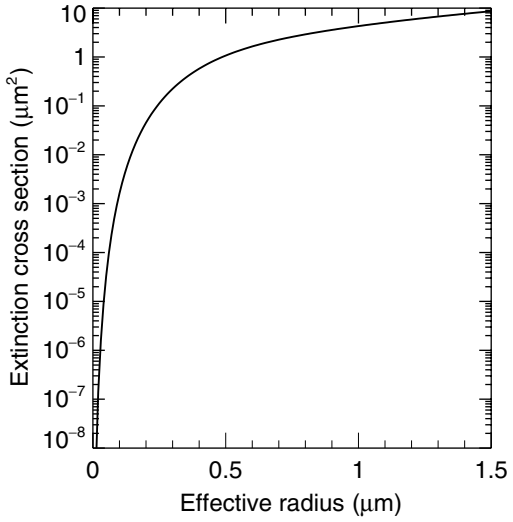

Fig. 2. Extinction cross section versus effective radius for a gamma distribution of spherical aerosols with $m = 1.45$ and $v_{\text{eff}} = 0.2$.

consideration that anticipated increases in the amount of greenhouse gases during the next 20 years will cause a forcing of about 1 Wm^{-2} [2].

The estimated plausible 20-year change of the global mean aerosol optical thickness is 0.04, whereas the global mean optical thickness change required to yield the 0.25 Wm^{-2} flux change is 0.01 [2]. These numbers imply that the accuracy for the aerosol optical thickness measurement should be the greater of ~ 0.02 or 7% over ocean and the greater of ~ 0.04 or 10% over land.

The accuracy for the aerosol size distribution retrieval (the greater of ~ 0.1 μm or 10% for r_{eff}; the greater of ~ 0.3 or 50% for v_{eff}) are dictated by the requirement to determine the aerosol number concentration with an accuracy sufficient for detecting the effect of increasing cloud condensation nuclei (CCN) concentration on cloud properties. The latter should be at least 30% or better [36]. Similarly accurate retrievals of the aerosol particle size are also needed in order to determine the cloud-condensation efficiency of aerosols [31,37].

The measurement accuracy for the real part of the aerosol refractive index (~ 0.015) is determined by the need to identify the aerosol chemical composition. The latter is required to identify hygroscopic aerosols, discriminate between natural and anthropogenic aerosol species, and estimate the imaginary part of the refractive index in order to provide an independent check on the retrieved single-scattering albedo.

The measurement accuracy for the cloud particle size distribution measurement (the greater of ~1 μm or 10% for r_{eff}; the greater of ~ 0.05 or 50% for v_{eff}) are dictated by the need to detect a flux change of 0.25 Wm^{-2} or greater [2], reliably detect a change of cloud particle size caused by increasing CCN concentrations [31–33], and determine the cloud droplet number concentration with an accuracy of at least 30%.

4. Hierarchy of passive remote-sensing instruments

Passive remote-sensing instruments measure the reflected solar radiation or the thermal radiation emitted by the atmosphere-surface system. The instruments based on measurements of the reflected sunlight can be classified

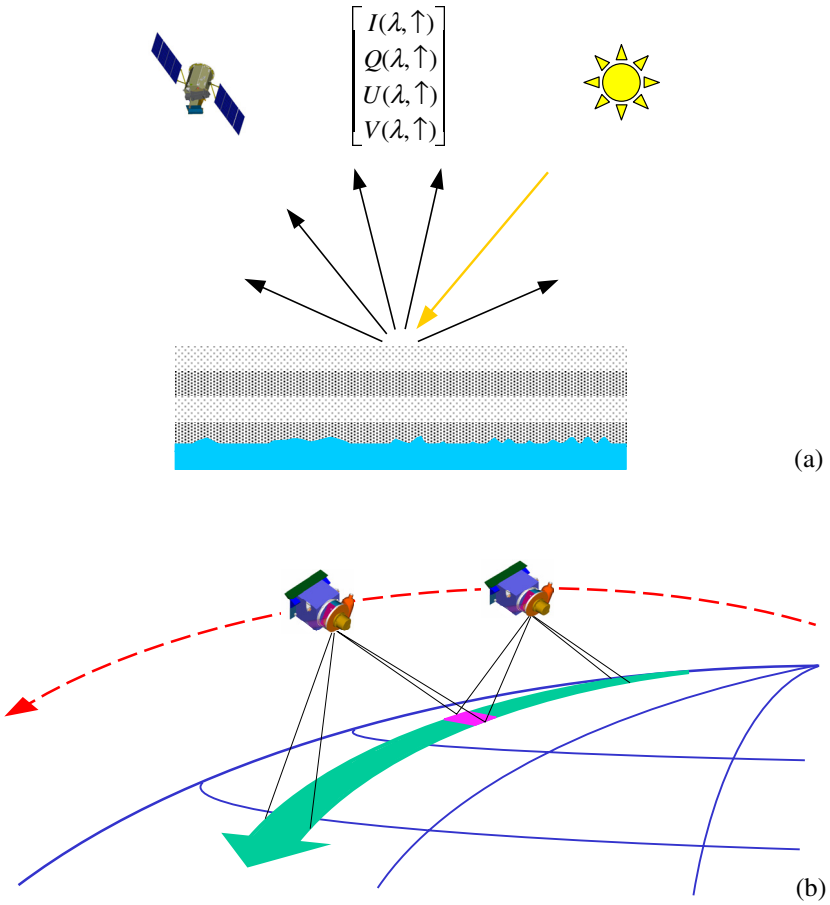

Fig. 3. (a) Classification of satellite instruments measuring various characteristics of the reflected sunlight. The Stokes parameters I, Q, U, and V of the reflected light vary with wavelength, λ, and scattering direction, $\uparrow$. (b) Along-track scanning photopolarimeter. By scanning along the ground track, the instrument observes the same piece of real estate from different viewing directions, thereby providing multi-angle measurements of the reflected radiance and polarization.

- by whether they measure only the radiance (i.e., the first Stokes parameter, I) or the radiance plus one or more of the remaining Stokes parameters describing the polarization state of the reflected radiation (i.e., Q, U, and V);
- by the measurement accuracy;
- by the number of spectral channels and the total spectral range covered; and
- by the number and range of viewing directions from which a scene location is observed

(see Fig. 3(a)).

At the bottom of the corresponding hierarchy of aerosol retrieval algorithms is the National Oceanic and Atmospheric Administration (NOAA) operational algorithm based on channel–1 Advanced Very High Resolution Radiometer (AVHRR) radiance data [13] and the NASA/GEWEX Global Aerosol Climatology Project retrieval algorithm based on channel–1 and –2 AVHRR radiance data [16].

The algorithms based on the Moderate Resolution Imaging Spectroradiometer (MODIS) [14,19] and the Multiangle Imaging Spectroradiometer (MISR) [18] data occupy intermediate positions. Indeed, both instruments measure only intensity, but have a significantly wider spectral range, especially MODIS.

Furthermore, MISR has the capability to look at the same ground pixel from several viewing directions.

The Polarization and Directionality of the Earth's Reflectance (POLDER) instruments [17] has the capability to measure the Stokes parameters Q and U as well as I, which makes it more advanced than the above-mentioned instruments. However, its spectral coverage is less wide that that of MODIS and the measurement accuracy for polarization is less than ideal.

At the top of the hierarchy of passive remote-sensing retrieval algorithms would be the one based on analyses of high-precision measurements of all four Stokes parameters taken in multiple spectral channels within a spectral range from near-UV to short-wave IR wavelengths and at multiple viewing directions covering a significant angular range.

The theoretical sensitivity analysis described in the following section as well as analyses of actual high-precision radiance and polarization data described in Section 7 and the publications cited therein show that retrieval algorithms based on radiance measurements alone cannot provide retrieval capability for some parameters or the accuracies summarized in Sections 3 and 4. The only instrument capable of retrieving aerosol and cloud properties with accuracy high enough for long-term monitoring of the aerosol radiative forcing would be a high-precision multi-angle photopolarimeter performing measurements at wavelengths from $\sim 0.4\,\mu m$ to $\sim 2.4\,\mu m$, Fig. 3(b) [34,38,39]. This instrument takes advantage of the strong sensitivity of the polarization state of sunlight reflected by the atmosphere to aerosol and cloud particle microphysics [26,40].

5. Sensitivity analysis

To illustrate the hierarchy of aerosol retrieval algorithms outlined in the previous section, we will now examine theoretically the ability of passive satellite instruments to provide an accurate retrieval of the requisite aerosol characteristics, in particular, the aerosol column density. For simplicity, we will consider only retrievals over the ocean surface since the ocean reflectance is low and can be rather accurately characterized. Our sensitivity analysis is based on numerically accurate calculations of polarized radiative transfer in a realistic atmosphere–ocean model [41] and theoretical simulations of several types of aerosol retrievals utilizing single-channel radiance and/or polarization measurements of reflected sunlight.

We follow the approach developed in [41] and use precomputed radiance, I, and normalized second and third Stokes parameters, $q = Q/I$ (%) and $u = U/I$ (%), for a large set of "candidate" aerosol models with effective radii r_{eff} varying from 0.005 to 0.8 μm in $0.005\text{-}\mu m$ increments, refractive indices m varying from 1.35 to 1.65 in steps of 0.005, and optical thicknesses τ ranging from 0 to 0.4 in steps of 0.005. The aerosol is assumed to be nonabsorbing, single-component, and monomodal with radii obeying a gamma size distribution with a fixed effective variance $v_{\text{eff}} = 0.2$. The analysis is restricted to a single near-IR wavelength $\lambda = 0.865\,\mu m$. The ocean surface roughness corresponds to the global average of the long-term annual mean wind speed (7 m/s).

We consider two strategies of single-channel satellite measurements, namely, what can be called the AVHRR strategy (reflectance and/or polarization measurements of a scene are performed at only one viewing angle) and the MISR strategy (employing multiple-viewing-angle radiance and/or polarization measurements of a scene). The illumination and viewing directions are specified by the cosine of the solar zenith angle μ_0 (fixed at 0.8), cosine of the satellite zenith angle μ, and relative satellite-sun azimuth angle φ. For the MISR type of measurements μ varies from 0.2 to 1 in steps of 0.2 in the satellite orbit plane specified by $\varphi = 60°$ and $-120°$, thereby yielding nine viewing directions covering the range of scattering angles from 82° to 148°. For the AVHRR type of measurements, the viewing direction is given by $\mu = 0.6$ and $\varphi = -120°$, thereby implying a scattering angle 103.9° in the same orbit plane.

Computer-simulated data includes the quantities I, q, and u for a "standard" aerosol model with $\tau_0 = 0.2$, $r_{\text{eff}} = 0.3$ μm, and $\mu_0 = 1.45$. We then assume that the aerosol model is unknown and attempt to reconstruct the "unknown" optical thickness, effective radius, and refractive index by comparing the reflectivity and/or polarization computed for the standard model with those for each of the candidate models from the large precomputed set.

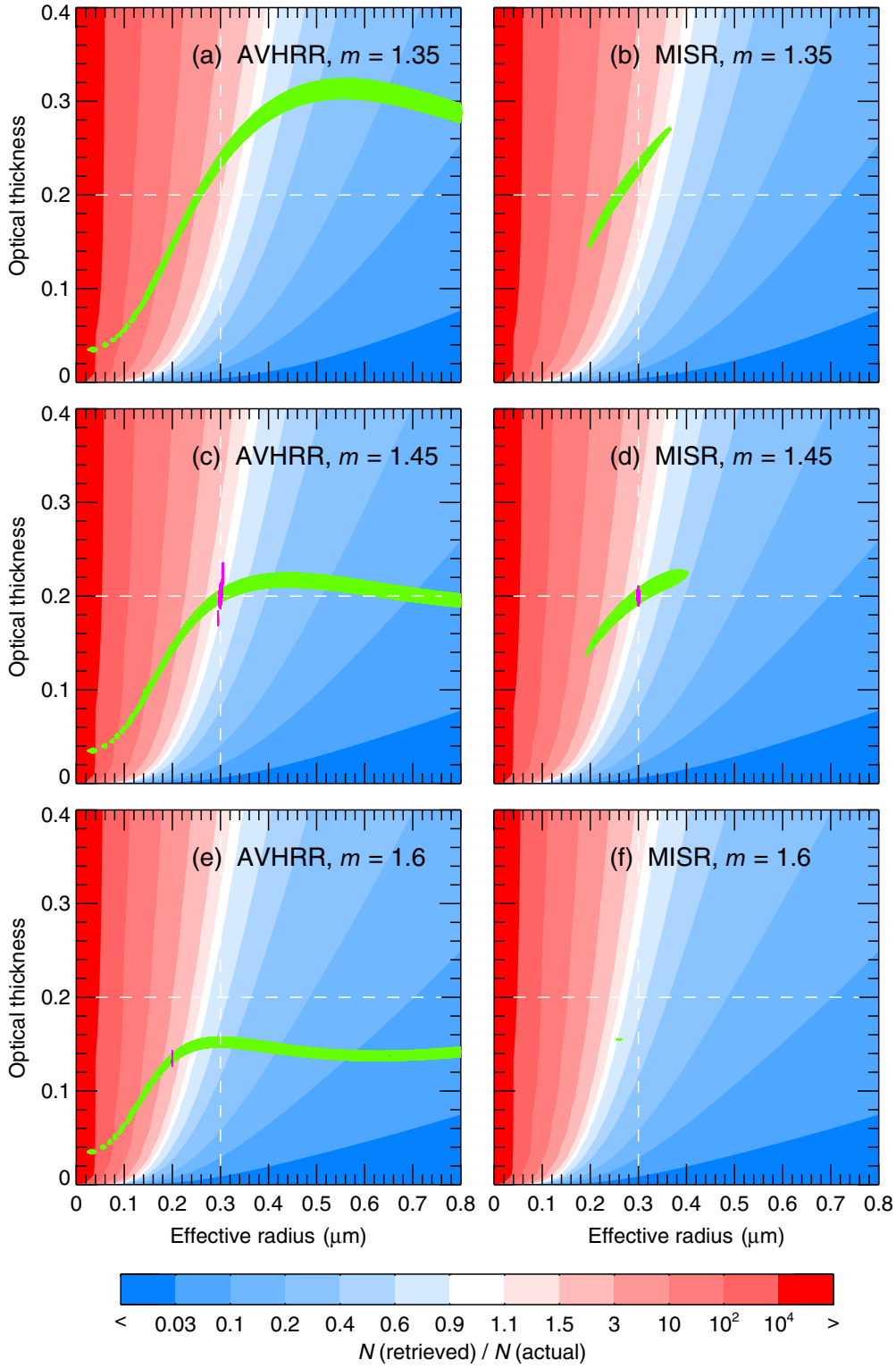

Fig. 4. Modeling different types of aerosol retrievals (see text).

We use three acceptance criteria which are intended to model retrievals using radiance measurements only (criterion A), polarization measurements only (criterion B), and radiance and polarization measurements combined (criterion C). The criteria select those candidate models for which the computed radiance and/or polarization do not deviate from those for the standard model by more than the assumed measurement errors. For the MISR type of measurements, the candidate–standard model deviations are averaged over the nine viewing directions. All candidate models that pass the acceptance criteria are equally good solutions so that none can be preferred as the unique retrieval.

The fact that the measurement errors in intensity and polarization never vanish results in multiple acceptable solutions. This is demonstrated in panels (a)–(f) of Fig. 4 computed for the AVHRR and MISR types of retrievals assuming radiance and polarization accuracies 4% and 0.2%, respectively. The intersection of the white dashed lines in panels (c) and (d) indicates the standard model (correct solution). The green color shows all candidate $(\tau, r_{\text{eff}}, m)$-combinations (for m = 1.35, 1.45, and 1.6) that passed the radiance-only acceptance criterion (A), the magenta color shows the result of applying the polarization-only criterion (B), and the intersections of the green and magenta areas show the result with criterion (C). The performance of the AVHRR type radiance-only algorithm is especially poor, the errors in the retrieved aerosol parameters τ, r_{eff}, and m being unacceptably large. This is not an unexpected result since it is hard to anticipate that an algorithm based on a single measurement can retrieve three unknown parameters with a high accuracy. That is why the actual NOAA AVHRR algorithm [13] is based on assuming rather than retrieving the aerosol model and retrieves only τ. However, panels (a), (c), and (e) clearly show that assuming wrong r_{eff} and m can result in very large errors in the retrieved optical thickness.

The use of nine measurements in the MISR type radiance-only algorithm, green areas in panels (b), (d), and (f), improves the retrieval significantly but still does not constrain all three aerosol parameters with the requisite precision. The latter is fully achieved only with the multiangle polarization algorithm, magenta area in panel (d). The absence of magenta areas in panels (b) and (f) demonstrates the sensitivity of the multiangle polarization algorithm to refractive index. The combined use of multiangle radiance and polarization, the intersection of green and magenta areas in panel (d), further improves the retrieval accuracy, but not much.

As we have mentioned before, errors in the retrieved optical thickness and assumed/retrieved aerosol model inevitably lead to errors in the retrieved aerosol column number density. The blue-and-red background in each panel of Figure 4 shows the possible range of the ratio of the retrieved to the actual aerosol column number densities for the different types of aerosol retrievals. Note that the color bar is strongly nonlinear and that the white color marks the regions where the ratio N(retrieved)/N(actual) does not deviate from unity by more than ±10%.

Panels (a), (c), and (e) show that the region of possible N(retrieved)/N(actual) values for the AVHRR type intensity-only algorithm spans many orders of magnitude, thus indicating that this type of retrieval is unsuitable for a reliable determination of the CCN column number density. The MISR type intensity-only algorithm provides a much better retrieval. However, even with this type of measurements the errors in the retrieved column density are much larger than in the other aerosol characteristics and can exceed a factor of 5. Only the multiangle polarization algorithm determines the aerosol model with such a precision that the retrieved aerosol column density is constrained to ±10%, panel (d).

An obvious limitation of this sensitivity analysis is that we considered only single-channel retrieval algorithms. The use of multispectral data from instruments like MODIS and MISR may be expected to improve the accuracy of radiance-only aerosol retrievals. However, our comparison of different remote-sensing techniques under exactly the same conditions clearly illustrates the tremendous improvement brought about by using high-precision polarimetric data in addition to radiance data.

6. GACP retrievals

Despite their obvious limitations, AVHRR instruments on board of NOAA weather satellites remain a unique source of information about aerosol properties owing to the extensive length of their combined

data record and the global coverage. Having this in mind, we have developed an aerosol retrieval algorithm based on analyses of channel–1 and –2 AVHRR data over the oceans [16,42–44] and applied it to the ISCCP DX radiance dataset [45]. Specifically, the algorithm retrieves the aerosol optical thickness τ and Ångström exponent A for each ISCCP pixel by minimizing the difference between two radiances measured in the 0.65-and 0.85-μm channels at the specific illumination and observation angles determined by the satellite orbit, on one hand, and the radiances computed theoretically for a realistic atmosphere–ocean model, on the other hand. The Ångström exponent is defined as

$$A = - \left. \frac{\mathrm{d}[\ln C_{\mathrm{ext}}(\lambda)]}{\mathrm{d}(\ln\lambda)} \right|_{\lambda=\lambda_1},$$

where $\lambda_1 = 0.65\,\mu\mathrm{m}$ is the nominal wavelength of the AVHRR channel 1 and C_{ext} is the ensemble-averaged extinction cross section per particle.

With only two pieces of data per pixel available, one can retrieve only the two model parameters and must assign fixed global values to the remaining parameters describing the complex atmosphere–ocean system, thereby introducing potential biases in the aerosol product. We have performed an extensive study of the expected accuracy of the algorithm and its sensitivity to various a priori assumptions [16,42] and have concluded that only averages of the optical thickness and Ångström exponent over a significant period of time (e.g., over a month) and over a significant area (e.g., over $1°\times1°$ pixels) can be expected to be reasonably accurate. Subsequent validation of GACP retrievals against extensive sunphotometer data [46] has corroborated this conclusion.

The two-channel AVHRR algorithm has been used in the development of a global climatology of the aerosol optical thickness and size for the period extending from July 1983 to September 2001 as part of the NASA/GEWEX GACP. The resulting product is posted on the world wide web at http://gacp.giss.nasa.gov/ retrievals. The extended aerosol record shown in Fig. 5 reveals no obvious long-term trend in the global mean optical thickness between the periods of major volcanic eruptions. This appears to provide a strong indication that there are no significant flaws in the radiance calibration used. Furthermore, the drift of the NOAA satellite orbits caused significant changes in the time of observation at a particular geographic location and, thus, in the illumination geometry over the period studied. Therefore, the absence of a pronounced long-term trend may also indicate that the accuracy of the ocean surface bidirectional reflectance modeling was sufficiently good and that the two-channel algorithm did a reasonably good job in terms of introducing no systematic bias in the aerosol retrievals.

The upper panel of Fig. 5 suggests that the average aerosol load tends to be greater in the Northern than in the Southern Hemisphere and that there is an annual variability pattern in the global average of the optical thickness with maxima occurring around January–February and minima in June–July. The Northern Hemisphere exhibits a similar pattern, but with maxima in February–April. One can clearly discern the residual effect of the El Chichon eruption (March 1982) in the form of increased optical thickness values in the beginning of the record. The June 1991 eruption of Mt. Pinatubo resulted in a sharp increase in the optical thickness to more than double its normal value. The temporal behavior of the constrained Ångström exponent (lower panel of Fig. 5) exhibits less regularity than that of the optical thickness. There seems to be a weak downward trend over the period studied, but it remains unclear whether it is real or is an artifact of residual radiance calibration drifts. The long-term mean aerosol optical thickness values obtained by averaging over the peroids not affected by major volcanic eruptions are 0.145 for the entire globe, 0.161 for the Northern Hemisphere, and 0.133 for the Southern hemisphere. The respective Ångström exponent averages are 0.75, 0.78, and 0.73.

Figure 6 illustrates the background levels of maritime aerosols found in the Northern and Southern Pacific Ocean and in the Southern Indian Ocean [47]. The borders of these regions were chosen so as to avoid the major influence of aerosols outflows from the continents. The Southern Pacific Ocean is one of the cleanest regions and has the aerosol optical thickness fluctuating around 0.1 during volcano-free periods. The Northern Pacific Ocean has a somewhat higher aerosol load, with a mean of 0.12, and

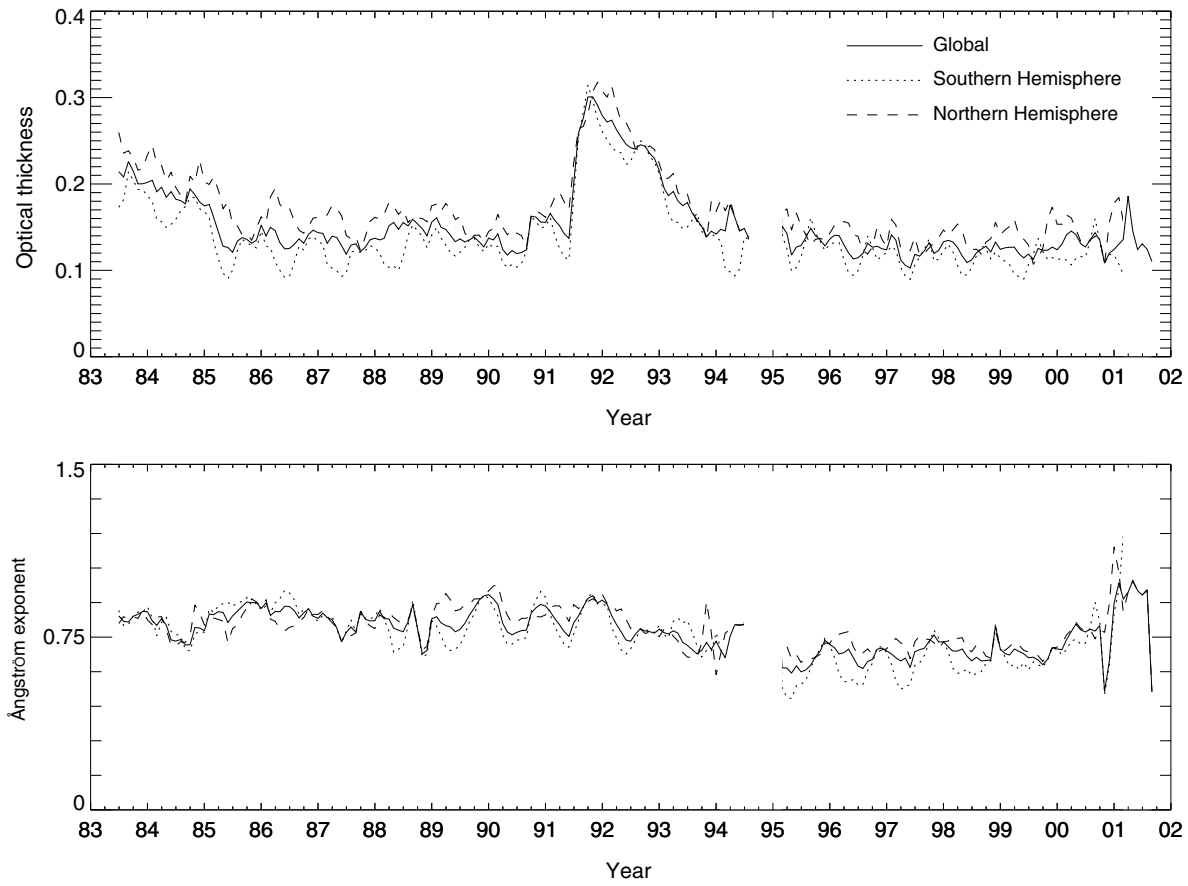

Fig. 5. Time series of the monthly global mean aerosol optical thickness and Ångström exponent retrieved from AVHRR channel–1 and –2 radiances.

slightly smaller particles (greater Ångström-exponent values) indicative of anthropogenic influence. The optical thickness record for the Southern Indian Ocean is similar to but slightly higher than that for the Southern Pacific Ocean, probably because of some residual dust contamination. The Ångström exponent is very close to that for the Southern Pacific Ocean and, as expected, is lower than that for the Northern Pacific Ocean.

7. Research Scanning Polarimeter retrievals

In the framework of the US Climate Change Research Initiative (CCRI; http://www.climatescience.gov/about/ccri.htm) launched in June 2001 to study areas of uncertainty about global climate change, research on atmospheric concentrations and effects of aerosols is specifically identified as a top priority. One of the activities that the CCRI calls out to support this research is improving observations for model development and applications from observing systems. To that end, the National Aeronautics and Space Administration (NASA) plans to deploy a high-precision photopolarimeter called Aerosol Polarimetry Sensor (APS) that will help understand the climate-relevant chemical, microphysical, and optical properties and spatial and temporal distributions of human-caused and naturally occurring aerosols. In addition to these science objectives, the Glory APS will be used to provide proof of concept and risk reduction for a nearly identical instrument to be flown by the US National Polar-Orbiting Operational

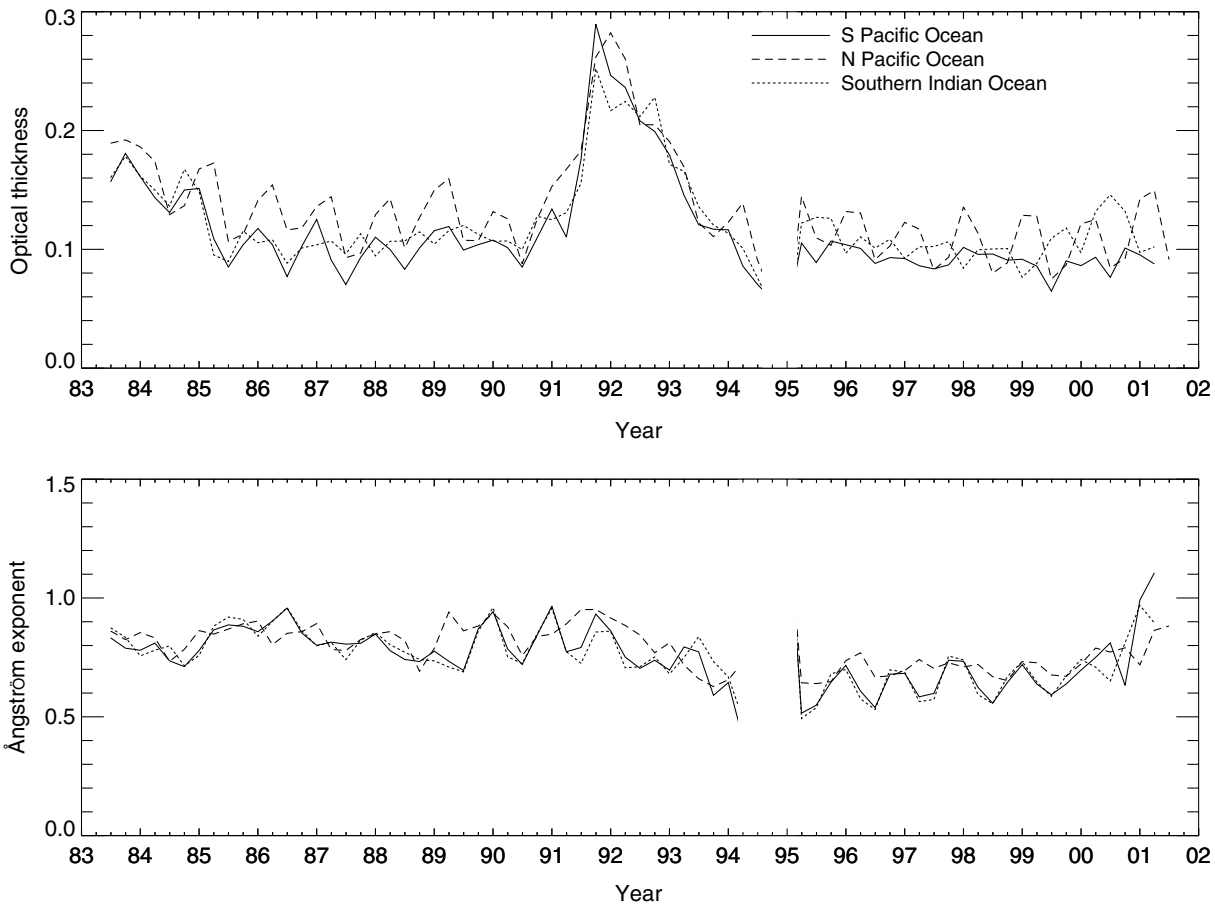

Fig. 6. As in Fig. 5, but for three distinct regions.

Environmental Satellite System (NPOESS) program (http://www.ipo.noaa.gov/Technology/aps_summary.html).

The APS shares many design features with the Earth Observing Scanning Polarimeter [48] and the Research Scanning Polarimeter (RSP) [49]. The latter is an aircraft instrument which has been used in several field campaigns [38,39,50] and can be expected to provide a close model of the future APS performance. Two examples of the fidelity of the aerosol optical thickness and size distribution estimated from this type of remote sensing measurement are shown in Fig. 7. In panel (a) the spectral optical thicknesses measured by ground-based sunphotometers are compared with those retrieved using polarimetric measurements [38]. The fact that the entire spectral range is well fitted in cases with both strong and weak spectral slopes is indicative of the reliability of the size distribution estimate for both small and large modes of a bi-modal aerosol distribution. Comparisons have also been made between in situ and retrieved size distributions and have also been found to agree extremely well (difference in effective radius of less than 0.04 μm).

The single-scattering albedo of aerosols can also be estimated from polarimetric measurements because of the differing sensitivity of polarized reflectance and unpolarized reflectance to aerosol absorption. In Fig. 7(b) [50] we show a comparison of the the estimated single-scattering albedo derived from polarimetric remote sensing measurements with *in situ* [51] and ground-based sky radiance [52] estimates of the single-scattering albedo. The discrepancy between these estimates may be related to the

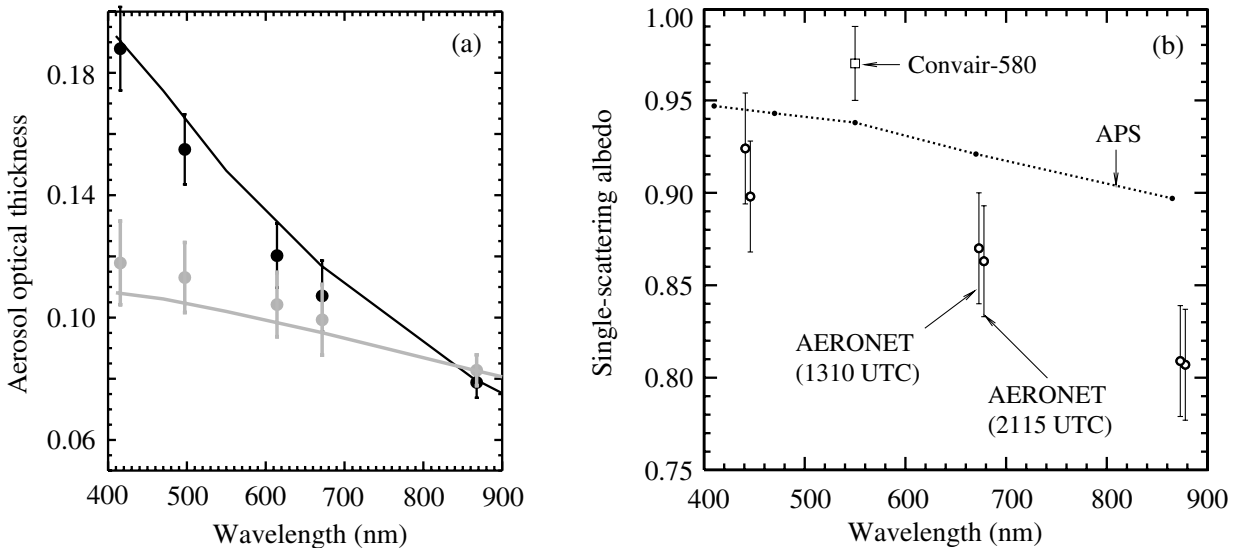

Fig. 7. (a) Optical depth comparison. Sunphotometer measurements for 14 October 1999 are shown as black filled circles and for 31 March 2000 as gray filled circles. Spectral dependence of aerosol optical depth inferred from polarimetry measurements on these two days are shown by the black and gray solid curves, respectively. Error bars are only shown for the sunphotometer measurements. (b) Single-scattering albedos as a function of wavelength. The dotted line shows the best-estimate values retrieved from RSP data. Also included are the estimates from data collected during Convair-580 flight 1874 and from the AERONET data.

loss of particles in the sampling system for *in situ* measurements, humidification of the *in situ* extinction coefficients (but not the absorption coefficients), and uncertainties in the retrieval of ϖ from AERONET data that may be caused by the considerable horizontal variability in the aerosol burden [51]. Nonetheless the polarimetric estimate of the single-scattering albedo is consistent with the other measurements given their inherent uncertainties.

In determining the effect of aerosols on clouds, it is essential that the cloud properties that are used do not have biases that depend on the type of cloud, or season. Existing methods for remotely determining the size of cloud droplets use the fact that the efficiency of liquid and ice absorption depends on particle size [53], or that the rainbow and glory features of radiation scattered by spherical particles are sensitive to particle size [54]. Methods using the efficiency of liquid and ice absorption must assume an effective variance of the droplet size distribution in their retrievals, which can cause biases in the estimated effective radius if incorrect [53]. Existing analyses of the rainbow and glory features in the radiation scattered by liquid water droplets are limited to very narrow size distribution widths for which these features have a large magnitude. This may cause serious sampling biases when trying to evaluate the effect of aerosols on clouds.

The APS sensor makes measurements that allow both methods to be combined and reduces their limitations [55]. Polarized reflectance measurements are sensitive to the droplet size distribution (effective radius and effective variance) in the top layer of the cloud (optical depth less than three) while the reflectance measurements in spectral bands where ice and water absorb (1.6 and 2.25 μm) are sensitive to a weighted integral through the depth of the cloud [56]. The type of measurements made by the APS therefore require a cloud model with two vertical layers. This allows the complete set of measurements to be matched with the additional benefit of providing sensitivity to the vertical profile of

droplet size and consequently reducing any biases in the estimated liquid water path and number density of droplets. In addition the polarized reflectance at scattering angles well separated from the rainbow and glory can be used to determine cloud top height [57] and the optical properties of haze above cloud top.

A good illustration of the performance of the RSP cloud algorithm is provided by comparison of the retrieved properties at cloud top with two *in situ* measurements obtained during the Coastal Stratocumulus Imposed Perturbation Experiment (CSTRIPE) on 25 July 2003 [55]. The APS retrievals of the cloud effective radius (9.75 μm), effective variance (0.2), and optical thickness (7.4) were an almost perfect fit to the respective *in situ* data: $r_{\text{eff}} = 9.75$ and 9.6 μm, $v_{\text{eff}} = 0.24$ and 0.18, and $\tau = 7.4$ and 7.4 (note that the *in situ* optical thickness estimates used a Gerber probe as the source for liquid water content). It is thus clear that not only is the cloud droplet effective radius accurately estimated, but also the effective variance of the droplet size distribution.

The droplet size estimates were in good agreement not only for the broad size distributions cited above but also for narrow size distributions on 22 July: 7.8 (0.8) and 8.7 (0.7) μm for effective radius and 0.04 (0.02) and 0.07 (0.015) for effective variance, where the first value is the RSP retrieval and the second one is an *in situ* measurement; the parenthetic values are the standard deviations for the 1 km samples. The optical thickness agreement was also extremely good: 13.99 and 13.955. Clearly given the sampling variability for the optical thickness estimates (3.05) this level (0.05) of agreement is fortuitous.

8. Implementation issues

At present, polarimeters designed for high-precision measurements (such as the EOSP, RSP, and APS) obtain the multi-angle coverage by scanning along the platform ground track (see Fig. 3(b)). The weakness of an along-track-scanning instrument is that it does not provide spatial coverage comparable to that of imagers such as MODIS, MISR, and POLDER. Therefore, the along-track-scanning multi-spectral photopolarimeter such as the APS should be flown in combination with a multi-spectral imager such as the Visible/Infrared Imager/Radiometer Suite (VIIRS; http://www.ipo.noaa.gov/Technology/viirs_summary.html). The photopolarimeter provides detailed aerosol information within a narrow swath along the ground track, which can be used to calibrate the imager retrieval algorithm and thereby obtain improved aerosol retrievals within the much wider swath of the imager. It can be argued that if the spectral radiances in all VIIRS channels within any continuous region of the VIIRS image are consistent with those predicted by the retrieved aerosol properties from the photopolarimeter, then the VIIRS-retrieved aerosol optical thickness and fraction of the fine mode aerosol are valid. While it is unlikely that such regions can extend to the edge of the VIIRS scan, i.e., 1500 km from the photopolarimeter ground track, it is expected that they often would extend to distances from the ground track significantly greater than 50 or even 100 km.

The quantification of the aerosol forcing and reducing its uncertainty may be an incomplete endeavor without an integrated approach that includes, in addition to space-based measurements, correlative measurements (from ground networks [58], aircraft [59–61], balloons, ships [62,63]) and modeling [7]. The correlative measurements can be used for validating satellite retrievals and can provide crucial information on the relationship between the aerosol chemical composition and the imaginary part of the refractive index (single-scattering albedo) [37,53]. Unlike space-borne measurements, the correlative measurements can provide direct information about physics and chemistry of aerosols and aerosol–cloud interactions [32,33,37]. The accuracy of aerosol and cloud modeling is the ultimate measure of our understanding of the processes that govern the formation, processing, and transport of aerosols and their interaction with clouds [7,64–66]. Furthermore, modeling can potentially be used to fill the gaps in the spatial and/or temporal coverage of satellite measurements.

Acknowledgements

This research was funded by the NASA Glory Project. Brian Cairns appreciates partial funding received from the NPOESS IPO.

References

[1] Hansen J, Sato M, Ruedy R, Lacis A and Oinas V 2000 *Proc. Natl. Acad. Sci. USA* **97** 9875
[2] Hansen J, Rossow W, Carlson B, Lacis A, Travis L, Del Genio A, Fung I, Cairns B, Mishchenko M and Sato M 1995 *Clim. Change*. **31** 247
[3] d'Almeida G A, Koepke P and Shettle E P 1991 *Atmospheric Aerosols* (Hampton, VA: Deepak)
[4] Seinfeld J H and Pandis S N 1997 *Atmospheric Chemistry and Physics: From Air Pollution to Climate Change* (New York: Wiley)
[5] Haywood J and Boucher O 2000 *Rev. Geophys*. **38** 513
[6] Penner J E et al 2001 *Climate Change 2001: The Scientific Basis*, ed J T Houghton et al (Cambridge: Cambridge Univ Press) p 289
[7] Hansen J, Sato M, Nazarenko L, Ruedy R, Lacis A, et al E 2002 *J. Geophys. Res.* **107** 4347
[8] Mishchenko M, Penner J and Anderson D ed 2002 *J. Atmos. Sci*. **59** 249
[9] Twomey S A 1991 *Atmos. Environ. A* **25** 2435
[10] Albrecht B A 1989 Science **245** 1227
[11] Hansen J and Nazarenko L 2004 *Proc. Natl. Acad. Sci.* **101** 423
[12] Kaufman Y J 1994 *Aerosol Forcing of Climate*, ed R J Charlson and J Heintzenberg (New York, Wiley) p 297
[13] Stowe L L, Ignatov A and Singh R 1997 *J. Geophys. Res.* **102** 16923
[14] Tanré D, Kaufman Y J, Herman M and Mattoo S 1997 *J. Geophys. Res*. **102** 16971
[15] Nakajima T and Higurashi A 1998 *Geophys. Res. Lett*. **25** 3815
[16] Mishchenko M I, Geogdzhayev I V, Cairns B, Rossow W B and Lacis A A 1999 *Appl. Opt*. **38** 7325
[17] Deuzé J L, Goloub P, Herman M, Marchand A, Perry G, Susana S and Tanré D 2000 *J. Geophys. Res*. **105** 15329
[18] Diner D J, Abdou W A, Bruegge C J, Conel J E, Crean K A, Gaitley B J, Helmlinger M C, Kahn R A, Martonchik J V, Pilorz S H and Holben B N 2001 *Geophys. Res. Lett*. **28** 3127
[19] Remer L A, Tanré D, Kaufman Y J, Ichoku C, Mattoo S, Levy R, Chu D A, Holben B, Dubovik O, Smirnov A, Martins J V, Li R-R and Ahmad Z 2002 *Geophys. Res. Lett*. **29** 10.1029/2001GL013204
[20] Coakley J A Jr, Bernstein R L and Durkee P A 1987 *Science* **237** 953
[21] Kaufman Y J and Fraser R S 1997 *Science* **277** 1636
[22] Mishchenko M I, Cairns B, Hansen J E, Travis L D, Burg R, Kaufman YJ, Martins J V and Shettle E P 2004 *J. Quant. Spectrosc. Radiat. Transfer* **88** 149
[23] Loeb N G and Kato S 2002 *J. Clim*. **15** 1474
[24] Christopher S A and Zhang J 2002 *Geophys. Res. Lett*. **29** 1859
[25] Francis P N, Hignett P and Taylor J P 1999 *J. Geophys. Res*. **104** 2309
[26] Hansen J E and Travis L D 1974 *Space Sci. Rev. 16* 527
[27] Kahn R, West R, McDonald D, Rheingans B and Mishchenko M I 1997 *J. Geophys. Res*. **102** 16861
[28] Masuda K, Mano Y, Ishimoto H, Tokuno M, Yoshizaki Y and Okawara N 2002 *Rem. Sens. Environ*. **82** 238
[29] Dubovik O, Holben B N, Lapyonok T, Sinyuk A, Mishchenko M I, Yang P and Slutsker I 2002 *Geophys. Res. Lett*. **29** 10.1029/2001GL014506
[30] Zhao T X-P, Laszlo I, Dubovik O, Holben B N, Sapper J, Tanré D and Pietras C 2003 *Geophys. Res. Lett.* **30** 1317.
[31] Schwartz S E, Blanchet J-P, Durkee P A, Hofmann D J, Hoppel W A, King M D, Lacis A A, Nakajima T, Ogren J A, Toon O B and Wendisch M 1994 *Aerosol Forcing of Climate*, ed R J Charlson and J Heintzenberg (New York, Wiley) p 251
[32] Brenguier J-L, Chuang P Y, Fouquart Y, Johnson D W, Parol F, Pawlowska H, Pelon J, Schuller L, Schroder F and Snider J 2000 *Tellus B* **52** 815

[33] Brenguier J-L, Pawlowska H and Schüller L 2003 J. *Geophys. Res*. **108** 8632
[34] Mishchenko M I, Travis L D, Rossow W B, Cairns B, Carlson B E and Han Q 1997 *Geophys. Res. Lett*. **24** 2655
[35] Feingold G 2003 *Geophys. Res. Lett*. **30** 1997
[36] Schwartz S E and Slingo A 1996 *Clouds, Chemistry and Climate*, ed P J Crutzen and V Ramanathan (Berlin: Springer) p 191
[37] Ogren J A 1994 *Aerosol Forcing of Climate*, ed R J Charlson and J Heintzenberg (New York, Wiley) p 215
[38] Chowdhary J, Cairns B, Mishchenko M and Travis L 2001 *Geophys. Res. Lett*. **28** 243
[39] Chowdhary J, Cairns B and Travis L 2002 *J. Amtos. Sci*. **59** 383
[40] Mishchenko M I, Travis L D, Lacis A A 2002 Scattering, Absorption, and Emission of Light by Small Particles (Cambridge: Cambridge Univ Press) (available at http://www.giss.nasa.gov/~crmim/books.html)
[41] Mishchenko M I and Travis L D 1997 *J. Geophys. Res.* **102** 16989
[42] Geogdzhayev I V, Mishchenko M I, Rossow W B, Cairns B and Lacis A A 2002 *J. Atmos. Sci.* **59** 262
[43] Mishchenko M I, Geogdzhayev I V, Liu L, Ogren J A, Lacis A A, Rossow W B, Hovenier J W, Volten H and Muñoz O 2003 J. Quant. Spectrosc. Radiat. Transfer. **79/80** 953
[44] Geogdzhayev I V, Mishchenko M I, Liu L and Remer L 2004 J. Quant. Spectrosc. Radiat. Transfer **88** 47
[45] Rossow W B and Schiffer R A 1999 *Bull. Am. Meteorol. Soc*. **80** 2261
[46] Liu L, Mishchenko M I, Geogdzhayev I, Smirnov A, Sakerin S M, Kabanov D M and Ershov O A 2004 *J. Quant. Spectrosc. Radiat. Transfer* **88** 97
[47] Geogdzhayev I V and Mishchenko M I 2005 in preparation
[48] Travis L D 1992 *Proc. SPIE* **1747** 154
[49] Cairns B, Travis L D and Russell E E 1997 *Proc. SPIE* **3220** 103
[50] Chowdhary J, Cairns B, Mishchenko M, Hobbs P, Cota G, Redemann J, Rutledge K, Holben B N and Russell E 2005 *J. Atmos. Sci.* in press
[51] Magi B I, Hobbs P V, Kirchsetter T W, Novakov T, Hegg D E, Gao S, Redermann J and Schmid B 2004 *J. Atmos. Sci.* in press
[52] Dubovik O, Holben B, Eck T F, Smirnov A, Kaufman Y J, King M D, Tanré D and Slutsker I 2002 *J. Atmos. Sci.* **59** 590
[53] Nakajima T and King M D 1990 *J. Atmos. Sci.* **47** 1878
[54] Breon F-M and Goloub P 1998 *Geophys. Res. Lett*. **25** 1879
[55] Cairns B 2005 in preparation
[56] Platnick S 2000 *J. Geophys. Res.* **105** 22919
[57] Goloub P, Deuzé J L, Herman M and Fouquart Y 1994 *IEEE Trans. Geosci. Rem. Sens.* **32** 78
[58] Holben B N, Eck T F, Slutsker I, Tanŕe D, Buis J P, Setzer A, Vermote E, Reagan J A, Kaufman Y J, Nakajima T, Lavenu F, Jankowiak I and Smirnov A 1998 *Rem. Sens. Environ*. **66** 1
[59] Russell P B, Hobbs P V and Stowe L L 1999 J. *Geophys. Res*. **104** 2213
[60] Russell P B and Heintzenberg J 2000 *Tellus B* **52** 463
[61] Clarke A D and Kapustin V N 2002 *J. Atmos. Sci*. **59** 363
[62] Bates T S, Quinn P K, Covert D S, Coffman D J, Johnson E J and Wiedensohler A 2000 *Tellus B* **52** 258
[63] Smirnov A, Holben B N, Kaufman Y J, Dubovik O, Eck T F, Slutsker I, Pietras C and Halthore R N 2002 *J. Atmos. Sci*. **59** 501
[64] Penner J E, Charlson R J, Hales J M, Laulainen N S, Leifer R, Novakov T, Ogren J, Radke L F, Schwartz S E and Travis L D 1994 *Bull. Am. Meteorol. Soc*. **75** 375
[65] Kiehl J T and Rodhe H 1994 *Aerosol Forcing of Climate*, ed R J Charlson and J Heintzenberg (New York, Wiley) p 281

[66] Ramaswamy V, Charlson R J, Coakley J A, Gras J L, Harshvardan, Kukla G, McCormick M P, Moller D, Roeckner E, Stowe L L and Taylor J 1994 *Aerosol Forcing of Climate*, ed R J Charlson and J Heintzenberg (New York, Wiley) p 385